Supporting Information

Entropic stabilization of RNA folding in crowded solutions measured by SAXS

Duncan Kilburn[1], Reza Behrouzi[1], Hui-Ting Lee[1], Krishnarjun Sarkar[1], Robert M. Briber[2*], Sarah A. Woodson[1*]

[1]T. C. Jenkins Department of Biophysics, Johns Hopkins University, Baltimore, MD 21218. [2] Department of Materials Science and Engineering, University of Maryland, College Park, MD 20742

Table S1. Magnesium-dependent folding of the Azoarcus ribozyme by SAXS. Data from Fig. 2. Errors from statistics of the fit; values of 0 indicate the parameter was held constant during the last stage of the fitting process.

55 °C	**0% PEG1000**	**10% PEG1000**	**18% PEG1000**
$C_{m,1}$ (mM)	0.25 ± 0.02	0.11 ± 0.05	0.13 ± 0.02
n_1	2.1 ± 0.2	1.8 ± 0.5	2.5 ± 0.2
$C_{m,2}$ (mM)	0.74 ± 0.01	0.45 ± 0.01	0.40 ± 0
n_2	7.6 ± 1.2	9.1 ± 1.2	13.3 ± 1.7
R_g U (Å)	79 ± 1	76 ± 1	73 ± 1
R_g I_U (Å)	48 ± 3	55 ± 3	51 ± 1
R_g I_C (Å)	30.5 ± 0.7	29.7 ± 0.3	29.3 ± 0.2
45 °C	**0% PEG1000**	**10% PEG1000**	**18% PEG1000**
$C_{m,1}$ (mM)	0.15 ± 0.02	0.17 ± 0.03	0.11 ± 0.02
n_1	2.0 ± 0.1	3.0 ± 0.4	2.6 ± 0.3
$C_{m,2}$ (mM)	0.55 ± 0.01	0.37 ± 0.02	0.29 ± 0.01
n_2	8.1 ± 0.9	8.5 ± 2.1	8.0 ± 1.5
R_g U (Å)	74 ± 1	70 ± 1	67 ± 1
R_g I_U (Å)	52 ± 2	49 ± 4	54 ± 3
R_g I_C (Å)	30.7 ± 0.3	30.0 ± 0.2	29.4 ± 0.2
37 °C	**0% PEG1000**	**10% PEG1000**	**18% PEG1000**
$C_{m,1}$ (mM)	0.16 ± 0.02	0.12 ± 0.02	0.05 ± 0.02
n_1	1.7 ± 0.1	2.8 ± 0.3	1.6 ± 0.3
$C_{m,2}$ (mM)	0.47 ± 0.01	0.34 ± 0.01	0.24 ± 0
n_2	7.7 ± 0.6	6.0 ± 0.7	4.8 ± 0.3
R_g U (Å)	64.1 ± 0.4	61.9 ± 0.4	59.8 ± 0.6
R_g I_U (Å)	47.8 ± 1.2	50.5 ± 2.1	54.0 ± 0.9
R_g I_C (Å)	30.7 ± 0.2	31.4 ± 0.1	29.8 ± 0.1

30 ˚C	**0% PEG1000**	**10% PEG1000**	**18% PEG1000**
$C_{m,1}$ (mM)	0.15 ± 0.05	0.11 ± 0.02	0.06 ± 0.02
n_1	1.8 ± 0.4	1.7 ± 0.1	1.5 ± 0.2
$C_{m,2}$ (mM)	0.36 ± 0.01	0.28 ± 0	0.2 ± 0
n_2	7.5 ± 1.5	7.0 ± 0.4	6.0 ± 0.4
R_g U (Å)	64.1 ± 0.9	59.3 ± 0.3	57.9 ± 0.3
R_g I_U (Å)	53 ± 3	51.8 ± 0.8	52.2 ± 0.8
R_g I_C (Å)	30.6 ± 0.3	30.2 ± 0.1	30.1 ± 0.1
25 ˚C	**0% PEG1000**	**10% PEG1000**	**18% PEG1000**
$C_{m,1}$ (mM)	0.14 ± 0.01	0.12 ± 0.02	0.10 ± 0.01
n_1	2.3 ± 0.1	1.8 ± 0.2	2.0 ± 0.1
$C_{m,2}$ (mM)	0.37 ± 0	0.25 ± 0	0.18 ± 0
n_2	7.9 ± 0.2	6.5 ± 0.6	5.0 ± 0.3
R_g U (Å)	60.2 ± 0.2	58.1 ± 0.3	56.2 ± 0.3
R_g I_U (Å)	50.0 ± 0	50.6 ± 1.3	50.0 ± 0
R_g I_C (Å)	31.3 ± 0.1	30.2 ± 0.1	30.3 ± 0.1
15 ˚C	**0% PEG1000**	**10% PEG1000**	**18% PEG1000**
$C_{m,1}$ (mM)	0.13 ± 0.01	0.08 ± 0.03	0.02 ± 0.03
n_1	3.6 ± 0.5	1.5 ± 0.3	1.4 ± 0.4
$C_{m,2}$ (mM)	0.33 ± 0	0.19 ± 0	0.14 ± 0
n_2	5.0 ± 0.1	4.4 ± 0.5	2.7 ± 0.2
R_g U (Å)	56.1 ± 0.2	57.0 ± 0.3	52.8 ± 0.4
R_g I_U (Å)	50.0 ± 0	51.2 ± 1.8	50.9 ± 1.5
R_g I_C (Å)	31.7 ± 0.1	30.4 ± 0.2	30.6 ± 0.2
5 ˚C	**0% PEG1000**	**10% PEG1000**	**18% PEG1000**
$C_{m,1}$ (mM)	0.15 0.01	0.05 0.32	0.03 0.1
n_1	5.4 0.9	1.9 1.1	3.0 0
$C_{m,2}$ (mM)	0.27 0.01	0.17 0.03	0.14 0
n_2	2.3 0.1	2.2 0.3	2.4 0.07
R_g U (Å)	54.5 0.2	52.4 0.3	50.2 0.4
R_g I_U (Å)	51.5 0	51 18	50.2 0.9
R_g I_C (Å)	31.0 0.1	30.4 0.2	30.4 0.1

Table S2. Thermodynamics and heat capacity change associated with ribozyme folding.[a]

PEG	ΔH°_{ref} (kcal/mol)	ΔC_p (cal/mol K)	ΔS°_{ref} (cal/mol K)
	0.2 mM $MgCl_2$		
0%	—[b]	—[b]	—[b]
10%	-35 ± 2	-1.5 ± 0.3	-120 ± 18
18%	-37 ± 3	-2.6 ± 0.4	—[b]
	0.3 mM $MgCl_2$		
0%	-24 ± 2	-0.7 ± 0.3	-83 ± 14
10%	-24 ± 1	-1.4 ± 0.2	-77 ± 20
18%	-21 ± 3	-1.9 ± 0.3	-64 ± 12
	0.4 mM $MgCl_2$		
0%	-20 ± 2	-1.2 ± 0.3	-66 ± 84
10%	-16 ± 2	-1.3 ± 0.3	-47 ± 8
18%	-9 ± 3	-1.5 ± 0.4	-23 ± 8

[a]The folding equilibrium constants in 0.3 mM $MgCl_2$ over the temperature range 10-55 ˚C were fit to

$$R\ln K = R\ln K_{ref} - \frac{\Delta H^o_{ref}}{T}\left(1-\frac{T}{T_{ref}}\right) + \Delta C_p\left(\frac{T_{ref}}{T} - 1 + \ln\left(\frac{T}{T_{ref}}\right)\right) \quad (3)$$

in which K_{ref} and ΔH°_{ref} are the equilibrium constant and enthalpy change at the reference temperature T_{ref} = 30 ˚C. ΔS°_{ref} was also evaluated at 30˚C. Errors are propagated from the statistical error of the fits.

[b]Could not be determined from the data.

FIGURE S1. Fraction of ATP modified by NMIA as a function of $MgCl_2$ concentration. Experiments were performed at 37 °C and 0% PEG. The mean value of two measurements is shown. Error bars are the absolute difference between these two measurements.

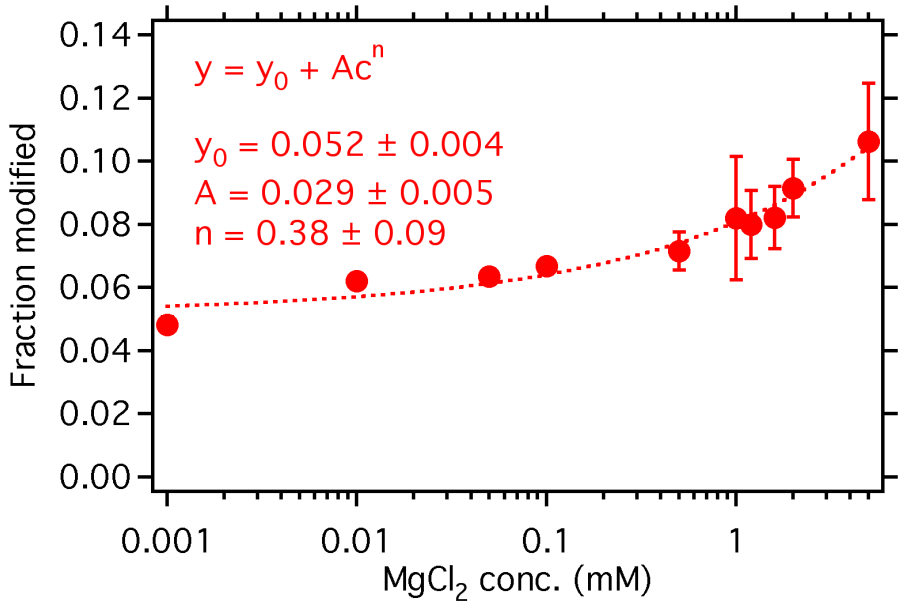

FIGURE S2. X-ray scattering functions of the *Azoarcus* ribozyme. Examples of small angle scattering functions used to monitoring ribozyme folding. Scattering of 0.4 mg/mL RNA in 20 mM Tris-HCl, pH 7.5 plus the desired $MgCl_2$ was measured as described in Materials and Methods. Curves represent the average of 4 data sets (1 s each). After subtraction of background scattering from the buffer or buffer + 18% PEG, scattering intensities in 18% PEG were scaled so that I(Q=0) is equal to I(0) in 0% PEG.

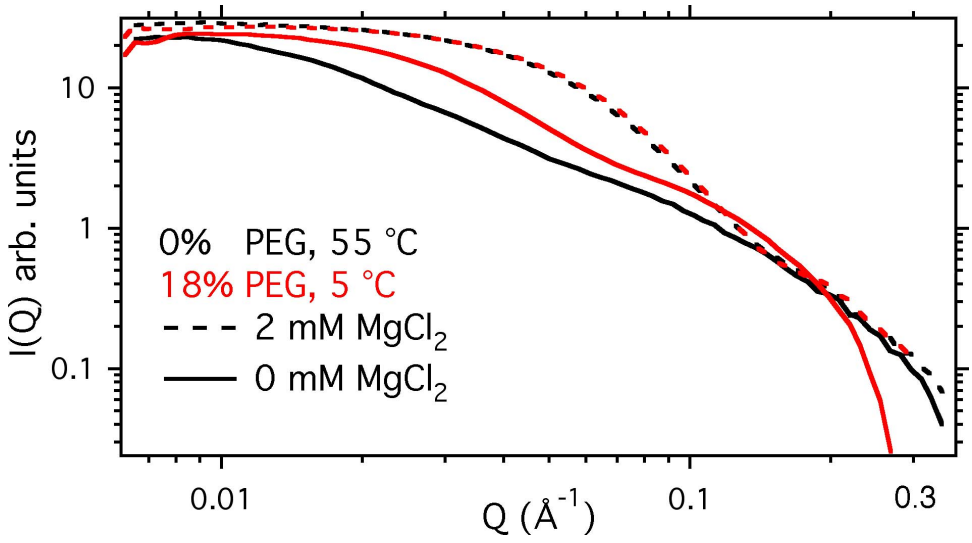

FIGURE S3. Density-density probability distribution functions for *Azoarcus* ribozyme molecules stabilized at 5 °C and 0%, 10% and 18% PEG for a)-c), respectively. RNA stabilized at 55 °C and 0%, 10% and 18% PEG is shown in d)-f), respectively. The different colors indicate RNAs stabilized in solutions containing a range of concentrations of $MgCl_2$ co-ions, from 0.01 mM (dark red) to 2 mM (magenta). The colors of the salt concentrations are given in the side bar. These probability distributions are calculated from SAXS scattering functions using GNOM and normalized to an equal area under the curve.

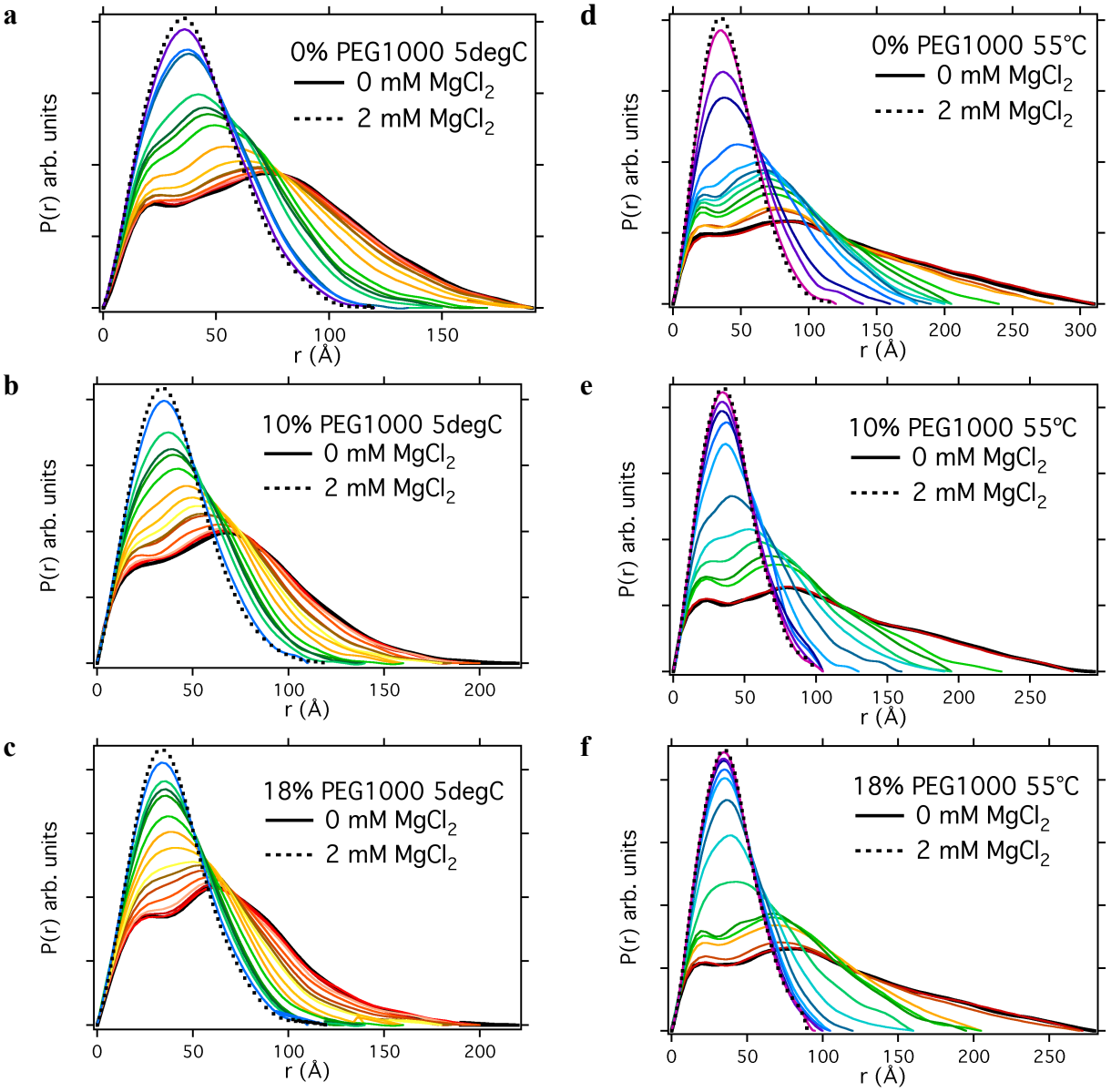

FIGURE S4. Contour plots of R_g as a function of Temperature and $MgCl_2$. a) In 0% PEG1000; **b)** n 18% PEG1000.

a)

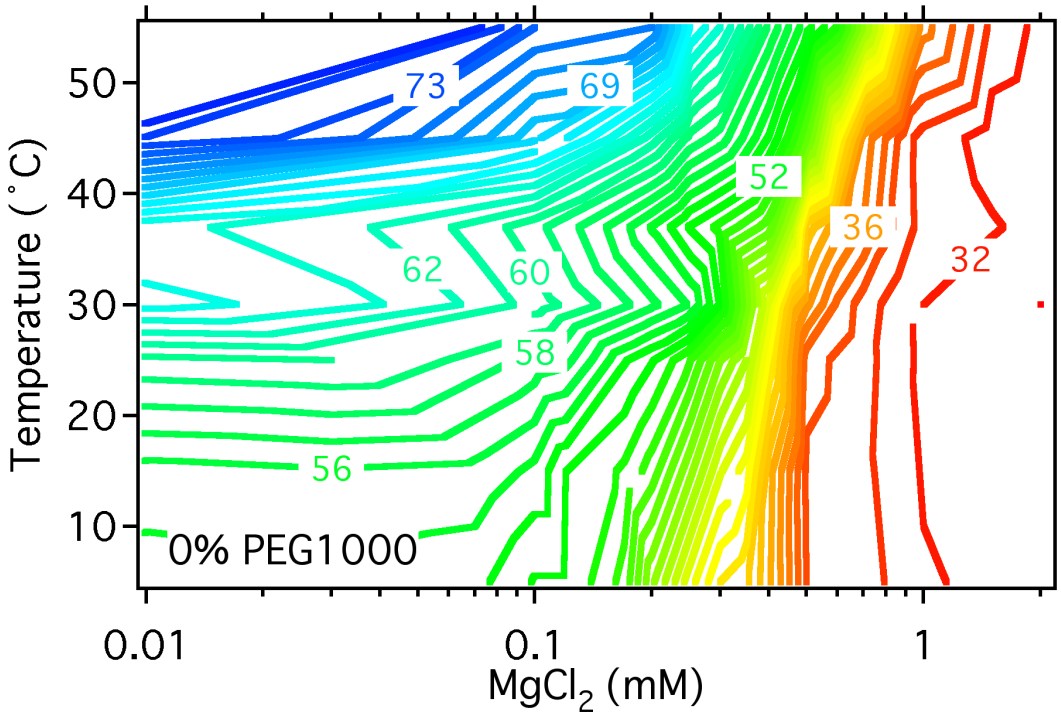

b)

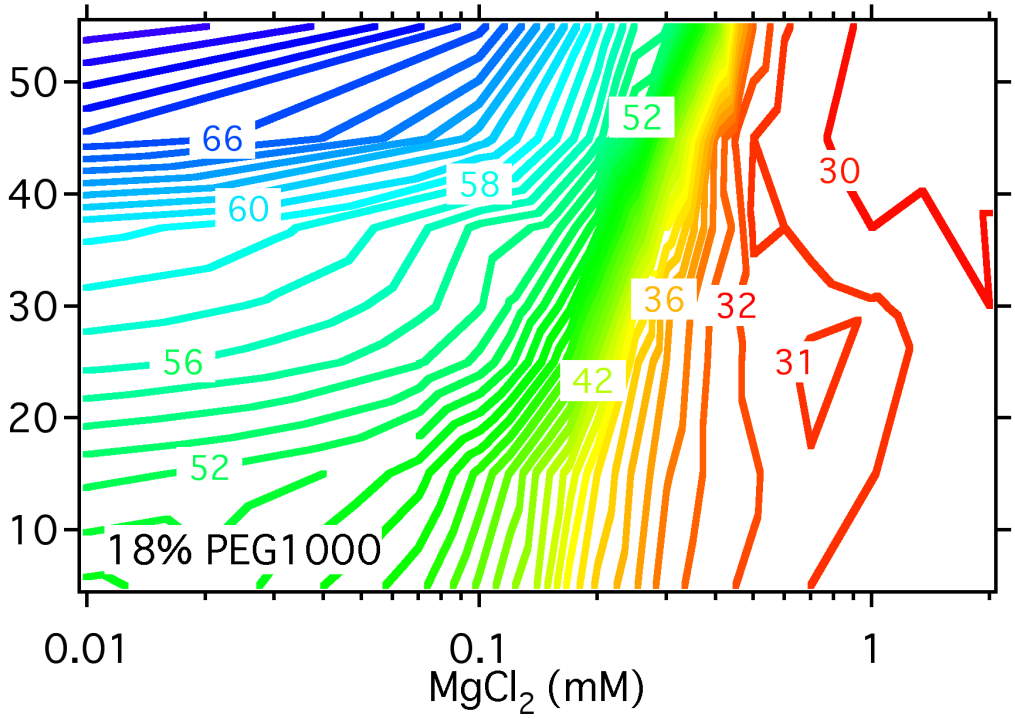

FIGURE S5. PEG shifts the Tm for helix assembly to lower Mg^{2+} concentrations. The fraction of native-like I_C intermediate versus temperature, in solutions containing no PEG (orange), 10% PEG (light blue) and 18% PEG (green). Data are for 0.3 mM $MgCl_2$ (closed symbols) and 0.4 mM $MgCl_2$ (open symbols). The fraction of I_C in each condition was calculated from the parameters in Table S1. Lines represent fits of the data to cooperative folding isotherms to estimate the midpoints for thermal denaturation of I_C in each solution condition. PEG reduces the $MgCl_2$ concentration required to achieve a particular Tm for the ribozyme tertiary structure.

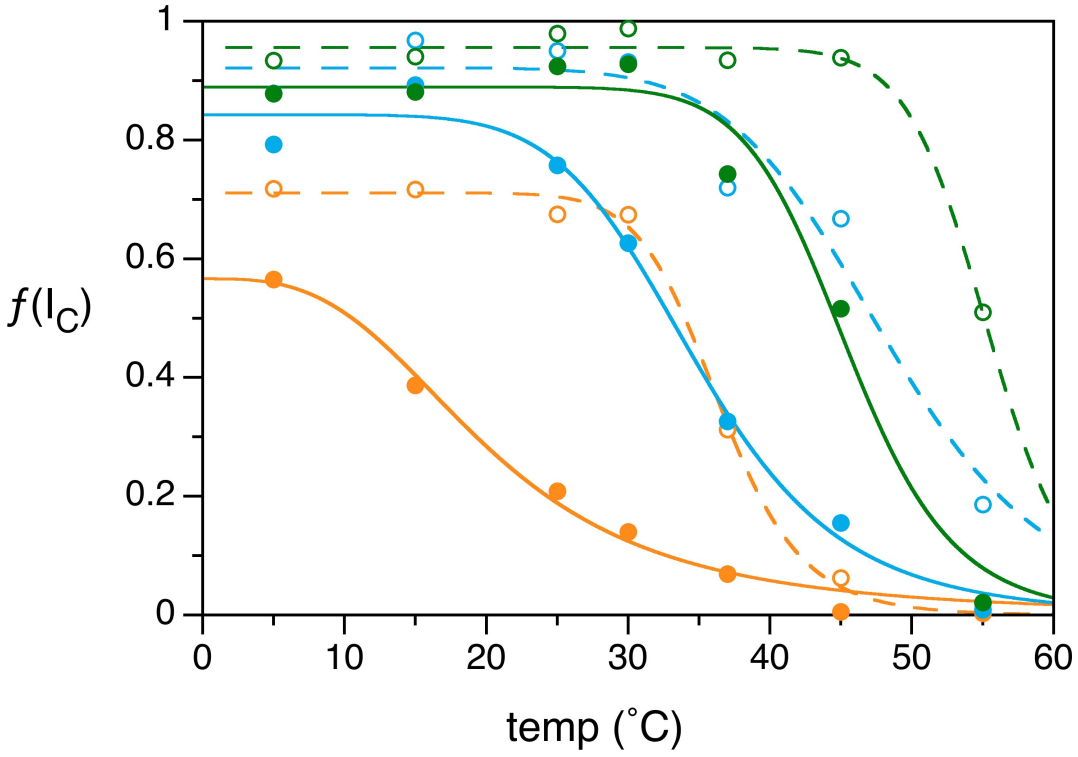

FIGURE S6. The radius of gyration of the semi-compact I_U state, $R_{g,I}$, vs. temperature in 0, 10 and 18% PEG. $R_{g,I}$ is determined from fits of Equation 1 and 2 to the data in Figure 2. $R_{g,I}$ is invariant on changing temperature and crowder level. Fitting constraints were imposed as described in figure 2: $R_{g,I}$, was constrained to have the same value at 5 °C: $R_{g,I}(0\%) = R_{g,I}(10\%) = R_{g,I}(18\%)$, but this was allowed to vary as a global fitting parameter. The value of $R_{g,I}(0\%)$ at 15 °C and 25 °C was fixed at 50 Å, which gave the most stable fits.

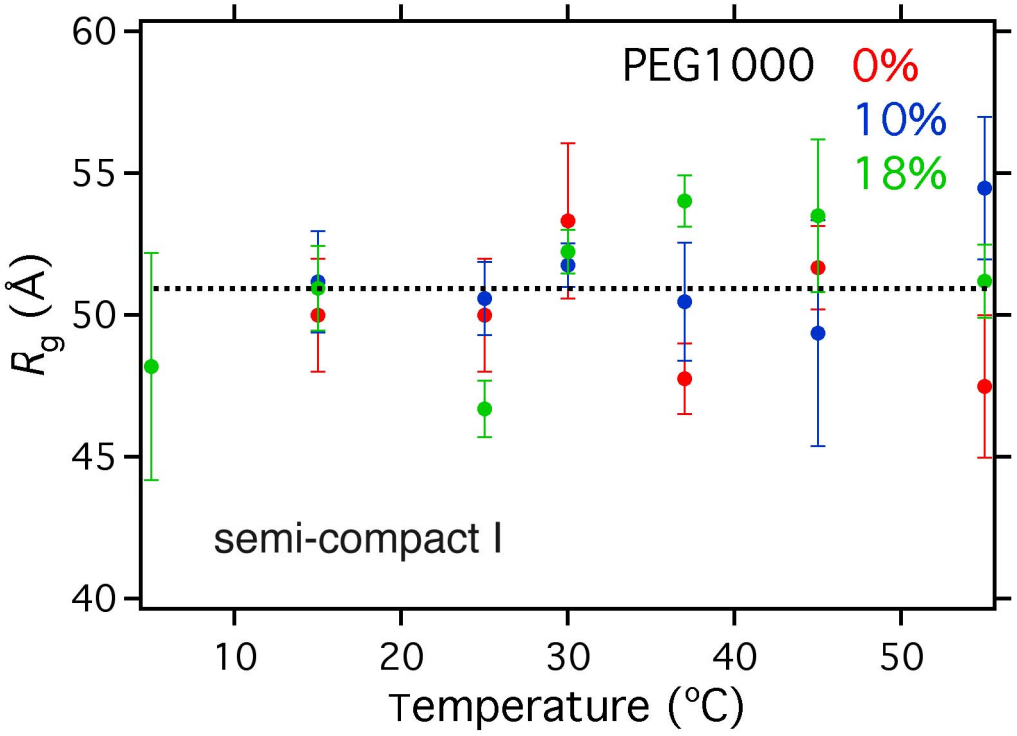

FIGURE S7. Temperature dependence of ribozyme folding. Linear van't Hoff plots in a) 10% PEG, b) 18% PEG.

a)

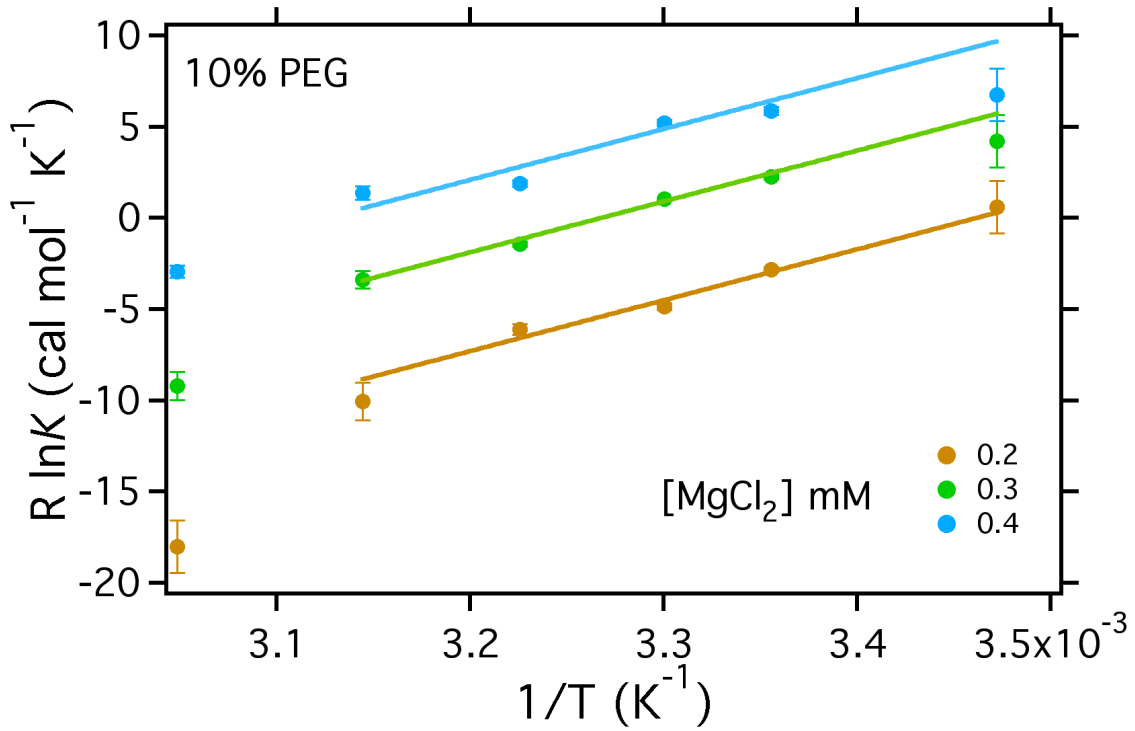

b)

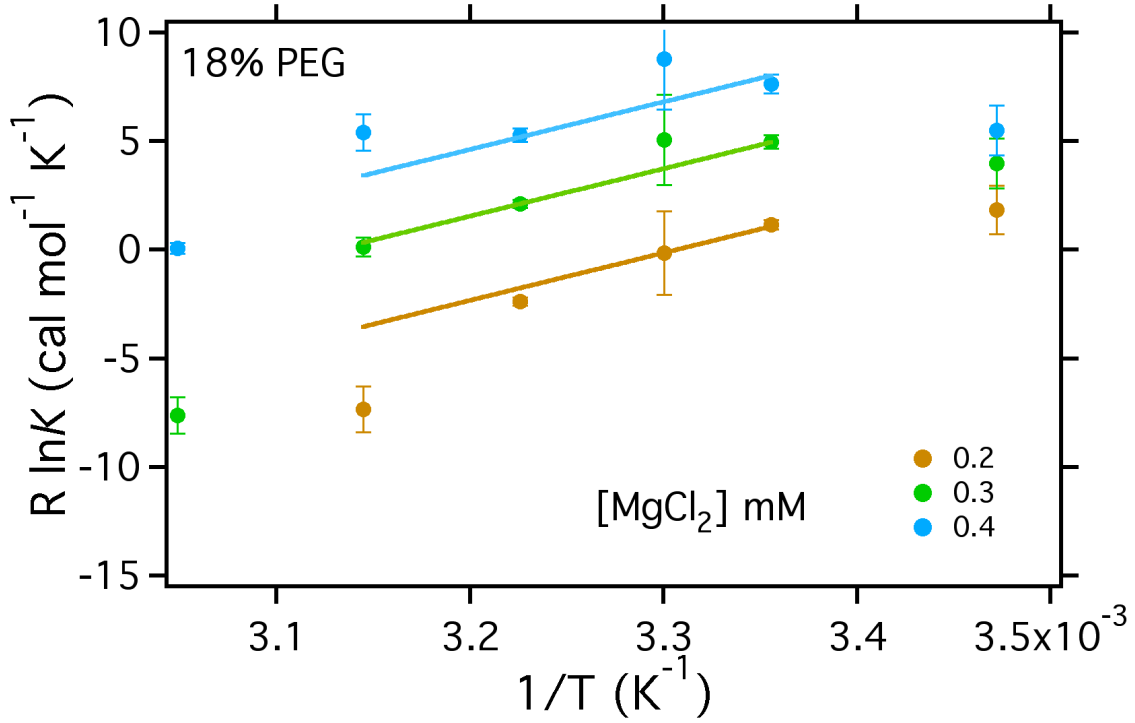

FIGURE S8. Folding equilibrium constant in 0.3 mM $MgCl_2$ vs. 1/T fit to eq. 3. Error bars propagated from the fits to Rg^2 vs. $MgCl_2$. Orange, no PEG, $\Delta C_p = -0.7 \pm 0.3$ kcal/mol K; green, 10% PEG1000, $\Delta C_p = -1.4 \pm 0.2$ kcal/mol K; blue, 18% PEG1000, $\Delta C_p = -1.9 \pm 0.3$ kcal/mol K.

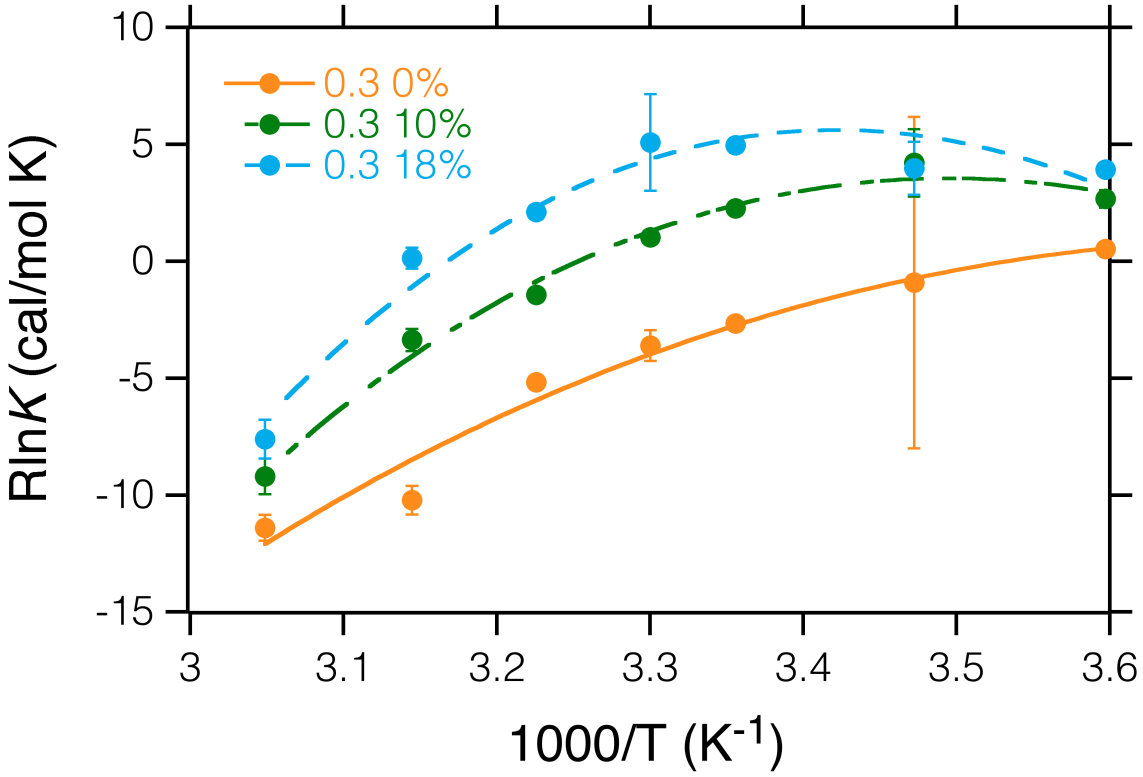

FIGURE S9. Comparison of Porod exponent versus radius of gyration for the *Azoarcus* ribozyme in buffer with 0 – 2 mM $MgCl_2$ at the temperatures given in the key. The radius of gyration, R_g, and the associated error was determined from P(r) distributions at each Mg^{2+} concentration as described in Methods. The Porod exponent ν was determined from linear fits to $\log I(q) = \log A - \nu \log q$ for q = 0.05 to 0.15 after subtraction of background scattering. Error bars represent the statistical quality of the fit.